JARO 18: 427–440 (2017)
DOI: 10.1007/s10162-016-0610-8

JARO
Journal of the Association for Research in Otolaryngology

Research Article

Deleting the HCN1 Subunit of Hyperpolarization-Activated Ion Channels in Mice Impairs Acoustic Startle Reflexes, Gap Detection, and Spatial Localization

James R. Ison,[1,2] Paul D. Allen,[3] and Donata Oertel[4]

[1]*Department of Brain and Cognitive Sciences, University of Rochester, Meliora Hall, Rochester, NY 14627, USA*
[2]*Department of Neuroscience, University of Rochester Medical Center, Rochester, NY 14642, USA*
[3]*Department of Otolaryngology, University of Rochester Medical Center, Rochester, NY 14642, USA*
[4]*Department of Neuroscience, School of Medicine and Public Health, University of Wisconsin, Madison, WI 53705, USA*

Received: 1 August 2016; Accepted: 14 December 2016; Online publication: 3 January 2017

ABSTRACT

It has been proposed that the high temporal and spatial acuities of human listeners and animals tested in the hearing laboratory depend in part on the short time constants of auditory neurons that are able to preserve or sharpen the information conveyed in the timing of firing of auditory nerve fibers. We tested this hypothesis in a series of in vivo experiments, based on previous in vitro experiments showing that neuronal time constants are raised in brainstem slices when HCN1 channels are blocked or in slices obtained from *Hcn1*$^{-/-}$ null mutant mice. We compared *Hcn1*$^{-/-}$ and *Hcn1*$^{+/+}$ mice on auditory brainstem responses (ABRs) and behavioral measures. Those measures included temporal integration for acoustic startle responses (ASRs), ASR depression by noise offset, and ASR inhibition by gaps in noise and by shifts of a noise source along the azimuth as measures of temporal and spatial acuity. *Hcn1*$^{-/-}$ mice had less sensitive ABR thresholds at 32 and 48 kHz. Their wavelet P1b was delayed, and wave 2 was absent in the 16 kHz/90 SPL waveform, indicating that groups of neurons early in the auditory pathways were delayed and fired asynchronously. Baseline ASR levels were lower in *Hcn1*$^{-/-}$ mice, temporal integration was delayed, time constants for ASR depression by noise offset were higher, and their sensitivity to brief gaps and spatial acuity was diminished. HCN1 channels are also present in vestibular, cutaneous, digestive, and cardiac neurons that variously may contribute to the deficits in spatial acuity and possibly in ASR levels.

Keywords: startle reflex, gap detection, maturation, sound localization, HCN1 null mutants

INTRODUCTION

Hyperpolarization-activated cyclic nucleotide-gated (HCN) channels are activated by hyperpolarization and provide a rectifying mixed-cation inward conductance (g_h) that is partially activated at rest and thus governs the input resistance of the cell and regulates its time constant (Moosmang et al. 1999; Wahl-Schott and Biel 2009). These tetrameric ion channels are assembled as homomers or heteromers of HCN1–4 subunits that vary in their kinetics and in their degree of modulation by cyclic nucleotides. The HCN1 subunits are the least regulated by cyclic nucleotides but have the fastest kinetics, and they are present at high levels in the membranes of many auditory neurons. These subunits are present in the hair cells of the cochlea and the vestibular utricle (Ramakrishnan et al. 2012; Horwitz et al. 2011) in the afferent dendrites, cell bodies, and axons of type I spiral ganglion cells (Mo and Davis 1997; Chen 1997; Bakondi et al. 2009; Yi et al. 2010; Kim and Holt 2013). They have been documented in bushy and octopus cells of the ventral cochlear nucleus (Bal and

Correspondence to: James R. Ison · Department of Brain and Cognitive Sciences · University of Rochester · Meliora Hall, Rochester, NY 14627, USA. email: jison@ur.rochester.edu

Oertel 2000; Koch et al. 2004; Oertel et al. 2008; Cao and Oertel 2011), in the lateral and medial superior olivary nuclei and the ventral and intermediate nuclei of the lateral lemniscus (Koch et al. 2004), in the superior paraolivary nucleus (Felix et al. 2014; Kopp-Scheinpflug et al. 2011), and in the inferior colliculus (Koch et al. 2004). HCN1 and HCN2 subunits (with the next fastest kinetics) are often present in the same channel, but not always (Koch et al. 2004).

In vitro electrophysiological experiments have shown that the kinetics and temporal precision of rapidly firing auditory neurons depend on the presence of HCN1 channels in the cell membrane (Banks et al. 1993; Felix et al. 2011; Kopp-Scheinpflug et al. 2011; Golding and Oertel 2012; Khurana et al. 2012). In many auditory neurons, the inward current that is mediated by HCN1 channels, I_h, is balanced by an outward, low-voltage-activated K^+ current, I_{KL}, and the conductances that underlie these currents contribute to the low input resistance and fast kinetics of auditory neurons (Manis and Marx 1991; Banks et al. 1993; Bal and Oertel 2000; Bal and Oertel 2001; Dodson et al. 2002; Khurana et al. 2011). The loss of HCN1 subunits not only results in a smaller and slower g_h but also results in a possibly compensatory smaller g_{KL} that maintains the resting potential of the cell but adds to the slowing of voltage changes. Other at least partial compensatory effects are possible, as have been noted in changes in neurotransmitter levels (Chen et al. 2010).

The auditory nuclei that express HCN1 subunits are linked in partially overlapping monaural and binaural pathways that provide the neural foundations for both temporal and spatial acuity, and thus, it is reasonable to expect that these sensory/perceptual abilities would be impaired by deleting HCN1.

METHODS AND PROCEDURES

Subjects

All of the mice in these experiments were the offspring of breeding pairs obtained from the Jackson Laboratory (Bar Harbor, ME): the *Hcn1*$^{-/-}$ mice were derived from three pairs of the B6129-*Hcn1*^{tndl}/J strain, while the *Hcn1*$^{+/+}$ mice were derived from three pairs of the B6129SF2/J strain that is described by Jackson as an approximate control for the null mutant mice. The backgrounds of these mice were identical to those used in a previous report (Cao and Oertel 2011). The two groups of mice had different physical and motor phenotypes: the *Hcn1*$^{-/-}$ mice were smaller, exhibited a head tilt and an unbalanced posture at rest, and poorly coordinated locomotion when moving around the home cage. These postural differences were apparent also in the *Hcn1*$^{-/-}$ mice tested by Kim and Holt (2013: personal communication, J. R. Holt, 2015). These experiments used a total of 76 *Hcn1*$^{+/+}$ mice (38 male, 38 female) and 70 *Hcn1*$^{-/-}$ mice (30 male, 40 female) with some included in more than one experiment. After weaning at about (Postnatal day) P25, groups of 3–4 same sex littermates were housed in the same cage, with the exception of within-strain breeding cages with one male/two female mice. The ambient noise level was 40 dB sound pressure level (SPL) at 2 kHz and declined linearly on the log-frequency scale to 25 dB SPL at 24 kHz. Sound levels were measured with a 0.25 in (6.5 mm) B&K microphone (model 4135) and sound level meter (model 2203, linear scale). The colony room temperature (21 °C) and humidity (70 %) levels were relatively stable, with little seasonal change. There was a 12/12 h normal light-dark cycle with testing during the day. The mice were deprived of food and water only in test sessions which lasted between 15 and 60 min in different experiments. In the longitudinal experiment, immature mice were removed from the litter for 15 to 20 min for testing and the chamber was heated to 25 °C by a heating pad to assure that pups could maintain their normal body temperature. All procedures were approved by the University of Rochester Committee on Animal Resources in accord with Public Health Service regulations and the Federal Animal Welfare Act.

Statistical Treatment of the Data

Descriptive statistics are reported as group means and standard error of the mean, as mean (SEM). These values and their graphic illustrations were provided by GraphPad PRISM software, version 7. The software also provided correlation coefficients between different conditions within groups, using the Spearman or Pearson *r* depending on the distribution of the data. Inferential statistics used for comparing two groups or two conditions within groups also used the GraphPad PRISM software, with Fisher's, Welch's, or the Mann-Whitney *t* test depending on the distribution of the data. Comparisons between several different groups or several different conditions within groups used the *F*-statistic provided by the ANOVA software SPSS (version 12), with within-subject repeated-measure comparisons using the Huynh-Feldt method for non-homogeneity of between-cell correlations. Degrees of freedom are given for each inferential statistic, e.g., $t(15)$ and $F(2,10)$. Effect size was provided by partial-eta-squared measures ($_p\eta^2$) after the ANOVA and R^2 after *t* tests.

Experiment 1: ABR Analysis, Threshold, and Waveforms

The details of the apparatus and procedures for auditory brainstem response (ABR) recording are described in Allen and Ison (2012). The mouse was anesthetized (ketamine/xylazine, 120 and 10 mg/kg) and placed in an electrically shielded, sound-attenuating chamber (Industrial Acoustics Company - IAC,

Bronx NY) clad with 3-in Sonex foam. Subdermal needle electrodes were placed at the vertex (reference electrode), over the bulla (active electrode), and above the hind limb (ground electrode). Tone pips (5 ms in duration, 0.5 rise/fall time at spectral frequencies of 3, 6, 12, 16, 24, 32, and 48 kHz, with a repetition rate of 10/s, and beginning 90 dB SPL) were provided by a electrostatic loudspeaker (TDT ES1) placed 10 cm in front of the mouse. Signal amplitude was automatically attenuated at each frequency in 5 dB steps until the positive wave complexes, P4 and P5, were no longer visually distinguishable: threshold was established as the just prior level. Average waveforms (150 repetitions × 2 replicates) were recorded at each tested frequency/amplitude combination. Stimulus presentation was under computer control, but latencies and amplitudes of the five peaks of the waveform produced by the 16 kHz/90 dB SPL test stimulus were analyzed offline. ABRs were measured in 9 male and 9 female mice $Hcn1^{+/+}$ mice, aged 63.56 (6.38) days and weighing 22.77 (1.32) g, and in 13 male and 5 female $Hcn1^{-/-}$ mice, aged 55.89 (2.80) days and weighing 18.78 (0.46) g. The difference in age was not significant ($p = 0.28$, $R^2 = 0.05$), but the weight difference was significant, Welch's $t(21.1) = 2.85$, $p = 0.01$, $R^2 = 0.28$.

Experiment 2: Temporal Resolution and Summation

Our behavioral apparatus and procedures for collecting acoustic startle response (ASR) data are described in Allen and Ison (2012). The apparatus was housed in a large IAC single-walled room (2.7 m long, 1.8 m wide and 2.4 m high). The walls and ceiling of the entire room were clad with echo-attenuating Sonex acoustical foam, as were the supports of speakers and animal's pedestal and the shelf to which the accelerometer was attached and the supporting table. The floor of the room was carpeted. All of the control equipment was placed in an adjacent room. The mice were tested one at a time in a small oval cage (5 cm × 7 cm × 4 cm high) mounted on a 15-cm pedestal that was bolted to an acrylic shelf attached to an accelerometer that was sensitive to the vertical force exerted by the startle reaction. The reflex-eliciting stimulus (ES) was provided by a real-time digital processor routed through programmable attenuators and passed to a TDT ES1 electrostatic speaker that was placed facing the test cage at a distance of 50 cm. The output of the accelerometer was rectified then integrated over a 100-ms interval beginning at the ES onset.

ASR-eliciting stimuli were presented in 14 conditions: (1) a single 12 kHz pulse with a duration of 1 ms; (2) a single 1 ms pulse with a 3-dB increment, considered here as a double pulse with an interstimulus interval (ISI) of 0 ms (ISI = 0); or(3) a single pulse with a duration of 2 ms, equivalent to two adjacent 1 ms pulses with ISI = 1; and then 11 conditions with 2 discrete pulses, with ISI of 1.5, 2,0 2.5, 3.0, 3.5, 4.0, 4,5, 5.0, then 6.0, 8.0 and 10.0 ms. All tone pips included 0.1 ms rise and fall times. Across days, the levels of the tone pips was set at 102, 105, 108, or 111 dB SPL, counterbalanced across days and mice. This additional variable of stimulus level was included because it was possible that the baseline ASR of the $Hcn1^{-/-}$ mice would be less than that of the $Hcn1^{+/+}$ mice, and if temporal integration had varied with the baseline amplitude, then comparisons between the groups would have been matched by their ASR amplitudes. The test days were separated by 3 or 4 rest days, with some few exceptions because of schedule conflicts. Twenty-five mice were used in this experiment, 12 $Hcn1^{+/+}$ mice (3 males, 9 females) aged 32.17 (0.85) days and weighing on the first test day 16.66 (0.84) g and 13 $Hcn1^{-/-}$ mice (5 males, 8 females) with age and weight being 34.23 (1.15) days and 14.19 (0.98) g. The difference in weight was of marginal significance, $p = 0.07$, $R^2 = 0.13$.

Experiment 3: Synaptic Depression After Noise Offset

The testing apparatus for this experiment and the general procedures are described in Ison and Allen (2012), differing from experiment 2 only in that the test apparatus was housed in a sound-attenuating anechoic chamber (Eckel Industries, Cambridge, MA) and there were two speakers: one was for the background noise, the other for the ES. The background noise had a level of 70 dB SPL and had programmable offset ramps ranging from 0 to 10 ms. The ES was a 110-dB SPL, 20-ms duration noise burst with 0 ms rise/fall times. The mice received baseline control trials with the ES presented in the presence of the continuous 70 dB noise and two types of trials in which the ES was presented just after noise offset, with noise offset leading the ES by intervals of 1, 2, 3, 4, 5, and 10 ms (ISI). On half of these trials, the offset was abrupt with a fall time of 0 ms, and on the other half, the offset followed a linear down ramp with the ramp time equal to the lead time (ramp type, RT; abrupt or gradual): for example, for an abrupt offset with an ISI of 10 ms, there was quiet period of 10 ms before the ES, while for a ramped offset with a duration of 10 ms, the ES was presented in quiet but at the end of the ramp. These conditions were presented in 11 blocks of trials, each block consisting of 14 trials in random order, included the six ISI conditions X two RT conditions, plus two control trials. A total of 41 mice was tested in this experiment, 20 $Hcn1^{+/+}$ (9 male, 11 female) at 43.80 (1.87) days of age and weighing 18.69 (0.53) g and 21 $Hcn1^{-/-}$ mice (5 male, 16 female) at 43.38 (2.00) days of age and weighing 15.34 (0.50) g. The difference in body weight was significant, $t(39) = 4.62$, $p < 0.001$, $R^2 = 0.35$.

Experiment 4: Gap Detection

The apparatus was the same as that described for experiment 3. The broad band background noise carrier for the gaps was set at 70 dB SPL, and the ES

was a 110 dB SPL noise burst with a 20 ms duration and abrupt rise and fall times. Because performance in gap detection experiments in juvenile rats increases with both increasing age and increasing experience with the stimuli (Dean et al. 1990), the first test on each day was a "pretraining" run with a suprathreshold test gap of 10 ms and the ES following the start of the gap by 10, 60, 100, 150, and 300 ms, or as a control, the ES presented in noise with no preceding gap. The gap detection test for thresholds followed after a rest of several hours in the home cage. The main test protocol presented gaps varying from 0 ms on control trials to 1, 2, 3, 4, 5, 6, 8, 10, or 15 ms, and in this experiment, the ES followed the end of the gap by a standard ISI of 60 ms.

The study began at P13 with 13 $Hcn1^{+/+}$ mice (7 male, 6 female) and 16 $Hcn1^{-/-}$ mice (8 male, 8 female). These mice were retested at P15 with the addition of three more $Hcn1^{-/-}$ mice, one male and two females. All were tested again at P17 (with the loss of data for one $Hcn1^{-/-}$ mouse) and again just before weaning at either P24, 25, or 26 (hereafter labeled as P25) with the full complement of 19 $Hcn1^{-/-}$ and 13 $Hcn1^{+/+}$ mice. The first adult test was given about 2 weeks after weaning, and a second test was given about 10 days later. An exclusion rule for the PPI data at any age was that the ASR control level must be significantly greater than the activity score, and for each adult mouse, the PPI data were used from their best performing day. The average age was 48.50 (2.14) days for the $Hcn1^{+/+}$ mice and 44.68 (1.24) days for the $Hcn1^{-/-}$ mice: the age difference was not significant, $R^2 = 0.09$. The mice were weighed on each test day, and these data are presented in the "RESULTS" section.

Experiment 5: the Minimal Audible Angle

The procedures for this experiment were adapted by Allen and Ison (2010, 2012) from an experiment by Mills (1958), in which blindfolded human listeners were presented with two successive tone pips from positions along the azimuth and asked if they were heard the second pip at the left or the right of the first: the smallest angular separation that could be detected with a 75 % correct criterion was the MAA, the "minimum audible angle." As adapted for mice and reflex inhibition audiometry, a continuous broadband test noise was presented from one of two speakers placed on the azimuth at different angles left and right across the midline, and a startle stimulus was presented at different intervals after the noise jumped from right to left or on control trials, presented with no preceding change in position. The MAA is the smallest angular separation at which a change in position significantly inhibited the ASR ($\alpha = 0.05$, one tail). The test room and apparatus used for experiment 2 was used again for this experiment with the addition of a second matched TDT ES1 electrostatic speaker. Both ES1 speakers were placed on a semicircular centered on the test cage at a distance of 50 cm. A third high-frequency speaker (JBL Model 075-105C) was mounted 12 cm above the test cage and provided the ASR eliciting stimulus, a 20-ms 120 dB noise burst with abrupt offsets and onsets. On each of the five test days, separated by two to five rest days, the two speakers were placed with angular separations of 90°, 45°, 22.5°, 15°, or 3.5°. The 3.5° test was a control condition to determine if the mice could detect a spectral difference between the two speakers. Each test day consisted of 11 blocks of trials with 13 conditions presented randomly in a block, consisting of 2 control trials (ES alone, with no prior change in position), and 11 trials in which the noise on the right hand speaker switched abruptly to the left hand speaker and the ES was then presented after one of 11 delays of 5, 10, 20, 30, 40, 50, 60, 100, 150, 200, or 300 ms. The return of the sound to the initial position for the start of the following trial was delayed for 2 s after the ES. Each testing session lasted approximately 60 min.

The main experiment (5A) on spatial acuity was designed to determine the MAA for $Hcn1^{+/+}$ and $Hcn1^{-/-}$ mice in broad band noise. It included 10 $Hcn1^{+/+}$ mice (6M, 4F) at an age of 45.6 (1.1) days and weight of 20.12 (1.05) g, and 12 $Hcn1^{-/-}$ mice (2M, 10F) at an age of 37.8 (0.8) days and a weight of 16.2 (0.41) g. The differences in both age and weight were significant: for age, $t(20) = 6.13$, $p < 0.001$, $R^2 = 0.65$, and for weight, $t(11.7) = 3.57$, $p < 0.01$, $R^2 = 0.52$. The mean ASR levels for the first test day was 6445.0 (808.8) aV-units for the $Hcn1^{+/+}$ mice and 6205.0 (583.0) aV-units for the $Hcn1^{-/-}$ mice: the difference in the ASR was not significant, $R^2 = 0.00$. The correlations of the ASR and weight were not significant for the 10 $Hcn1^{+/+}$ mice, $r = +0.25$, but significant for the $Hcn1^{-/-}$ mice, $r = +0.66$, $p = 0.02$. The second experiment (5B) was designed to determine if the deficit in spatial acuity in the $Hcn1^{-/-}$ could be attributed to their high frequency hearing loss shown in Fig. 1a. This experiment compared the performance of $Hcn1^{+/+}$ and $Hcn1^{-/-}$ mice when either a 48-kHz low pass noise or a 24-kHz low pass noise was displaced by 45° across the midline: if the high-frequency octave band from 24 to 48 kHz was critical for the better performance of the $Hcn1^{+/+}$ mice in experiment 5, then the performance of the two strains should be identical for the 24-kHz low pass noise in experiment 5B. The subjects were 15 $Hcn1^{+/+}$ mice (11M, 4F) at 49.5 (2.9) days of age and a body weight of 20.67 (0.87) g, with 11 naïve mice and 4 mice carried over from experiment 4, and 15 $Hcn1^{-/-}$ mice (4M, 11F) at 46.40 (3.03) days of age and a body weight of 16.67 (0.72) g, with 9 naïve mice and 6 mice carried over. There were significant differences in the control baseline ASR, summing over the two spectral

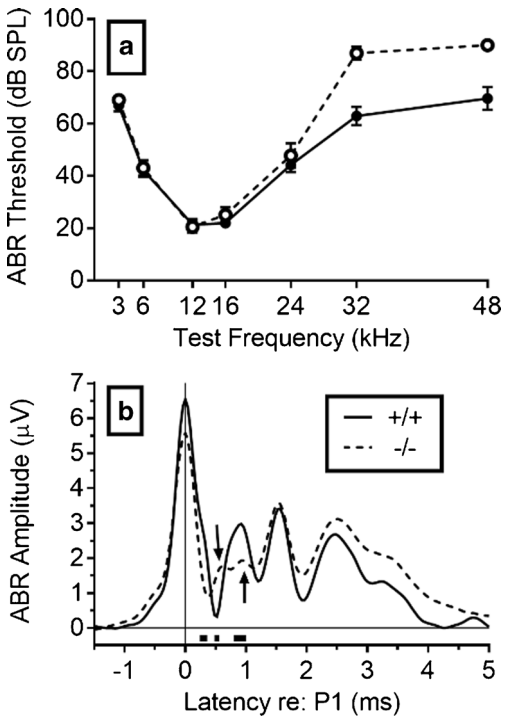

FIG. 1. Experiment 1. **a** ABR thresholds are shown for the *Hcn1*$^{+/+}$ mice in *solid symbols* and *continuous lines* and for the *Hcn1*$^{-/-}$ mice in *open symbols* and *broken lines*. The *Hcn1*$^{-/-}$ mice had a ~20 dB hearing loss above 24 kHz, but even the *Hcn1*$^{+/+}$ mice had a ~30 dB hearing loss at those frequencies compared to C3HeB/FeJ mice, the background for *Kcna1* knockouts (Allen and Ison 2012). **b** The mean ABR mean amplitudes at 16 kHz and 90 dB SPL are shown for the *Hcn1*$^{+/+}$ mice in a *continuous line* and for the *Hcn1*$^{-/-}$ mice in the *broken line*, with the time scale set at P1 = 0. The latency of P1 was exactly the same in the two strains, but they diverged in the falling phase of P1. The *three rectangular blocks* under the abscissa between latencies of ~0.2 to 1 ms after P1 show the time points at which the amplitudes were significantly different ($p < 0.05$). The *first arrow* at a latency of about 0.5 ms points to a delayed P1b for the −/− group, and the *second arrow* at about 1 ms points to their reduced P2.

conditions for the 15 *Hcn1*$^{+/+}$ mice, 2327.6 (215.6) aV-units, and for the 15 *Hcn1*$^{-/-}$ mice, 1042.0 (177.2) aV-units, $t(28) = 4.60$, $p < 0.001$, $R^2 = 0.43$. There were no significant correlations between body weight and baseline ASR in either group, $R^2 = 0$.

Experiment 6: Motor Coordination and Balance

The apparatus for measuring motor coordination and vestibular function was made up of a stationary elevated metal rod, 50 cm long with a diameter of 1.2 cm, and mounted 40 cm above the floor of an acrylic tank, 50 cm long and 25 cm wide. The floor was covered with foam batting. The apparatus was housed on a table in a sound-attenuating IAC test room and was illuminated by an overhead light. Each litter of mice to be tested was transported from the vivarium to the test room in its home cage. Each mouse had just one test trial. It was gently picked out of home cage and placed by hand across the rod at its center. A timer began when the mouse was released and was stopped when it fell off. Our results were based on measurements of six male and four female *Hcn1*$^{+/+}$ mice with a mean age of 44.0 (1.0) days, weighing 18.85 (0.77) g, and seven male and six female *Hcn1*$^{-/-}$ mice aged 46.6 (1.2) days weighing 16.93 (0.60) g. The difference in age was not significant, $p = 0.12$, $R^2 = 0.11$, and the weight difference was of marginal significance, $p = 0.06$, $R^2 = 0.16$.

RESULTS

Experiment 1

The aims of this experiment were to determine whether HCN1 deletion would alter ABR thresholds and possibly change the shape of the ABR waveform as a direct indication of impaired auditory processing. Kim and Holt (2013) had found no effect of HCN1 deletion on either ABR thresholds (up to 32 kHz) or on the amplitude of the first peak of the waveform (P1: auditory nerve), but they did find a modest delay in P1 latency. However, their background mice and their presentation rate were different from ours. Our ABR thresholds are presented in Fig. 1a. The two groups were nearly identical from 3 to 24 kHz, but the thresholds at 32 and 48 kHz were about 20 dB SPL higher in the *Hcn1*$^{-/-}$ mice: Welch's $t(22.3) = 7.95$, $p < 0.001$, $R^2 = 0.74$. The ABR waveforms at 16 kHz and 90 dB SPL for the *Hcn1*$^{+/+}$ and *Hcn1*$^{-/-}$ mice are shown in Fig. 1b. The latency of P1 was calculated for each mouse beginning from the time of entrance of the test tone into the external auditory meatus, and then for the group data shown in Fig. 1b, the waveform of each mouse was aligned so that its P1 was 0 ms. Aligning P1 removes individual differences in P1 that are generated in the peripheral spiral ganglion and thus provides temporal information about central delays in the ascending neural pathways of the auditory brainstem. The latencies at this peak were identical in the two groups, with a mean latency of 1.26 (0.01) ms for the *Hcn1*$^{+/+}$ mice and 1.26 (0.02) ms for *Hcn1*$^{-/-}$ mice. The mean amplitude of P1 for the *Hcn1*$^{+/+}$ mice was 6.54 (0.72) μV compared to 5.57 (0.42) μV for the *Hcn1*$^{-/-}$ mice, but this difference was not significant, $p = 0.26$, $R^2 = 0.05$. The earliest significant difference between the two groups was observed in the rapid decay of P1 to an apparent earlier N1 in the *Hcn1*$^{-/-}$ mice, at a mean latency of 0.39 (0.21) ms compared to 0.50 (0.15) ms in the *Hcn1*$^{+/+}$ mice, $t(33) = 4.04$, $p < 0.001$, $R^2 = 0.33$. However, inspection of the individual waveforms

suggested that this difference reflects a delayed P1b in the *Hcn1*$^{-/-}$ mice. The P1b "shoulder" for P1 is generated by auditory nerve activity after its emergence from the internal meatus (note the first arrow pointing to P1b). While being only a subtle inflection in wild type mice, it is a distinctive feature for humans and cats because of their longer AN (Starr and Zaaroor 1990; Melcher and Kiang 1996). The most conspicuous effect of HCN1 deletion in Fig. 1b was the near absence of the second peak, P2, in the *Hcn1*$^{-/-}$ mice (note the second arrow pointing at P2). P2 reflects the synchronous firing of groups of cells in the anteroventral nucleus of the cochlear nucleus (CN) (Henry 1979; Melcher and Kiang 1996). The loss of P2 in the *Hcn1*$^{-/-}$ mice indicates that these mice have abnormal temporal firing patterns, and this effect by itself may be expected to affect behavior in tests of temporal and spatial acuity.

Up to 16 kHz, the absolute thresholds for both *Hcn1*$^{+/+}$ and *Hcn1*$^{-/-}$ mice shown in Fig. 1a approximate the threshold levels reported by Kim and Holt (2013) for their similar test frequencies. However, the thresholds at 24 and 32 kHz were less sensitive by 20 to 30 dB SPL than those of Kim and Holt (2013) even for our *Hcn1*$^{+/+}$ mice, and for our *Hcn1*$^{-/-}$ mice, these thresholds were further increased by an additional 20 dB SPL. There were some differences in the ABR procedures, as noted above, but a more interesting possibility is that the different outcomes reflect the backgrounds of the mice, which is not an unusual effect (Crawley et al. 1997). Their mice had a predominant C57BL6 background, ours a mixed C57BL6 and 129SF background. The 129SF strain has an very early high frequency hearing loss (Yoshida et al. 2000) that may have been exacerbated by the deletion of *Hcn1*, as HCN1 channels are normally present in hair cell stereocilia (Ramakrishnan et al. 2012).

Experiment 2

This experiment was developed from an early study on temporal acuity in the auditory system by Exner (1875: described by William James 1890), in which two clicks were presented and the listener reported hearing one or two clicks: the threshold was ~2 ms. A similar experiment with rats used two brief startle-eliciting tone pips found maximum summation at 3 ms and a possible threshold at 2 ms (Marsh et al. 1973). For our data, Fig. 2a shows that the ISI that generated the peak ASR was consistently at ~2 ms and 1.5 ms earlier in the *Hcn1*$^{+/+}$ mice across stimulus levels. The overall mean ISI that generated peak ASRs was 2.09 (0.08) ms for the *Hcn1*$^{+/+}$ mice and 3.61 (0.18) ms for the *Hcn1*$^{-/-}$ mice. The ANOVA of these data showed that only the effect of gene deletion was significant, $F(1/23) = 52.51$, $p < 0.001$, ${}_p\eta^2 = 0.70$. Figure 2b shows the mean amplitude of the

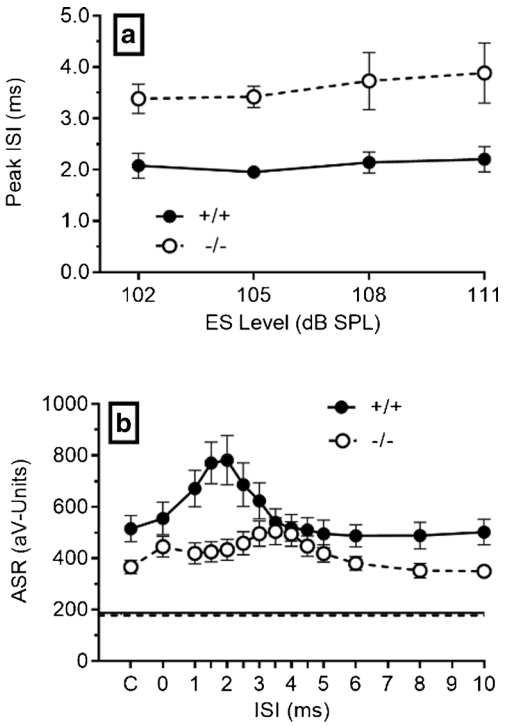

FIG. 2. Experiment 2. **a** The best interval (ISI) for temporal integration of the ASR given two brief (1-ms) tone pips was delayed in the *Hcn1*$^{-/-}$ mice by about 1.5 ms for each of the stimulus levels. **b** The mean ASR amplitude is shown at each ISI summed across all intensities. These data show the more robust summation effect of the double-pulse stimuli in *Hcn1*$^{+/+}$ mice compared to the *Hcn1*$^{-/-}$ mice. In contrast, the effect of the increased intensity of the single stimulus at ISI = 0 was evident in both groups.

ASR at each ISI for the two groups summed over each stimulus level and including also the mean activity scores on control trials. The baseline ASR for the *Hcn1*$^{+/+}$ mice was greater than that of the *Hcn1*$^{-/-}$ mice, Welch's $t(16.44) = 2.60$, $p < 0.05$, $R^2 = 0.29$, while activity scores were not different, $p = 0.49$, $R^2 = 0.01$. The ANOVA of these data provided a significant effect for ISI, $F(3/299) = 17.99$, $p < 0.001$, ${}_p\eta^2 = 0.44$, and a significant interaction between ISI and gene deletion, $F(3/299) = 11.55$, $p < 0.001$, ${}_p\eta^2 = 0.33$. The ASR amplitude of the *Hcn1*$^{+/+}$ mice significantly increased from ISI = 1 ms to the peak at ISI = 2 ms, $t(11) = 3.79$, $p = 0.003$, $R^2 = 0.57$. For the *Hcn1*$^{-/-}$ mice, the increase in the ASR from the ISI of 1 ms to their peak ISI at 3.5 ms was of marginal significance, $t(12) = 2.13$, $p = 0.055$, $R^2 = 0.27$, while in contrast, temporal integration for the *Hcn1*$^{+/+}$ mice had completely dissipated at the 3.5 ms ISI. A two-way ANOVA comparing the single pulse control with the ISI of 3.5 ms in the two groups provided a significant interaction, $F(1/23) = 5.57$, $p = 0.03$, ${}_p\eta^2 = 0.20$. After their peak values, the decrement in the ASR amplitudes of both groups was well described by exponential decay functions having different time constants and 95 %

confidence intervals: for the $Hcn1^{+/+}$ mice, τ = 1.05 ms (0.83–1.42 ms), and for the $Hcn1^{-/-}$mice, τ = 2.02 ms (1.23–5.19 ms): resolution of the two stimuli and summation of their excitatory responses were slower to develop and to dissipate in $Hcn1^{-/-}$ mice.

Experiment 3

The goal of this experiment was to determine whether the latency of the depressive effect of noise offset on the ASR is longer in $Hcn1^{-/-}$ mice, an effect that may reflect adaptation in hair cells (Fettiplace and Kim 2014) or the synaptic depression at stimulus offset in the in vitro studies on the cochlear nucleus (Wang and Manis 2008; Yang and Xu-Friedman 2009). In this experiment, the mean baseline ASR for the $Hcn1^{+/+}$ mice was 3262.0 (225.8) aV-units, and for the $Hcn1^{-/-}$ mice, 1425.0 (133.6). This difference was significant, with Welch's $t(39) = 7.08$, $p < 0.01$, $R^2 = 0.61$. The within-group correlations between body weight and ASR amplitudes were near zero, with $R^2 = 0.01$ for the $Hcn1^{+/+}$ group and $R^2 = 0.07$ for the $Hcn1^{-/-}$ group, and neither body weight nor the baseline ASR levels were significantly correlated with the levels of response depression produced by noise offset. There were no differences in background activity between the two groups: for the $Hcn1^{+/+}$ mice, 311.6 (9.7), and for the $Hcn1^{-/-}$ mice, 285.0 (14.0) aV-units: $p > 0.10$, $R^2 = 0.06$. The major results of this experiment are given in Fig. 3. Plots of the relative depression of the ASR in $Hcn1^{+/+}$ and $Hcn1^{-/-}$ mice with abrupt vs. ramped offsets and various lead times are fitted with best-fit exponential regression lines for each condition. Consistent with prior experiments in young adult mice (Ison and Allen 2012), the critical duration between the abrupt and the ramped conditions for the $Hcn1^{+/+}$ mice was less than 1 ms, and the difference between the abrupt and the ramped offset at 1 ms was significant, $t(19) = 3.69$, $p = 0.002$, $R^2 = 0.52$. Response depression developed more slowly in $Hcn1^{-/-}$ mice: the difference between the abrupt vs. gradual offset first appeared at the 2 ms interval, with $t(20) = 4.21$, $p = 0.004$, $R^2 = 0.47$. At the 1-ms interval, the difference of the abrupt vs. ramped offsets between the two groups was significant, $t(39) = 2.14$, $p = 0.04$, $R^2 = 0.47$, but they were not significantly different at 2 ms, $t(39) = 0.03$, $R^2 = 0$. Conversely, at the 10-ms lead time, the difference between the abrupt and ramped offsets was greater in the $Hcn1^{-/-}$ mice, $t(39) = 2.26$, $p = 0.03$, $R^2 = 0.12$, suggesting greater perseveration of the behavioral effects of abrupt and ramped offsets in these mice. The more slowly developing response depression in the $Hcn1^{-/-}$ mice is evident also in the regression lines in Fig. 3, given by a one-stage exponential association model that accounted for 95 to 98 % of the variance of the means in each condition. For the $Hcn1^{+/+}$ mice, the time constant and its 95 % confidence limit for the abrupt offset was τ = 2.44 ms (2.14–2.85) and for the gradual ramped offset, τ = 4.82 ms (4.19–5.63). For the $Hcn1^{-/-}$ mice, the time constant for the abrupt offset was τ = 4.09 ms (3.89–4.76) and for the ramped onset, τ = 8.28 ms (7.02–10.11). The time constants for the ramped offsets were twice those for the abrupt offsets for both groups, and the time constants for the $Hcn1^{-/-}$ mice were about twice those for the $Hcn1^{+/+}$ mice. These data agree with those of experiment 2 in showing that HCN1 deletion delays the initial behavioral effect of an acoustic stimulus but is then followed by longer perseveration of its effect. The rapidity of the behavioral effect of noise offset in the $Hcn1^{+/+}$ mice indicates that its neural foundation in the ASR pathway as synaptic depression in the cochlear root nucleus (CRN) and in their ipsi- and contralateral pathways to the caudal pontine reticular formation and, from there, to the cranial and spinal motoneurons, as described by Gomez-Nieto et al. (2014).

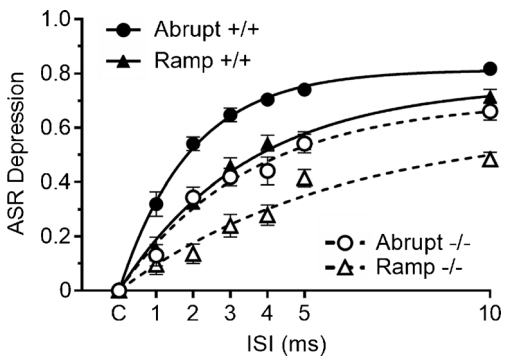

FIG. 3. Experiment 3. The separation of the effects of abrupt and gradual offsets on the ASR was slower in $Hcn1^{-/-}$ mice than in the $Hcn1^{+/+}$ mice. The best-fit exponential growth functions are depicted for each condition. The time course of the $Hcn1^{+/+}$ mice for abrupt compared to ramped offsets was τ = 2.4 vs. 4.8 ms, but these values for the $Hcn1^{-/-}$ mice were 4.1 vs 8.3 ms.

Experiment 4

This experiment was done to determine whether deletion of HCN1 affects the threshold for gap detection, a function that is correlated with speech recognition, most obviously in neurology patients with peripheral auditory neuropathy (Zeng et al. 2005; Michalewski et al. 2005) or bilateral lesions in the auditory cortex (Buchtel and Stewart 1989) but also in listening in noisy conditions for normal elderly listeners (Snell et al. 2002). An additional goal was to examine the physical status and behavior in $Hcn1^{-/-}$ mice at ages common for in vitro work and then to extend the analysis into adulthood. Figure 4 shows the development of body weight, ASR amplitudes, and activity levels from P13 to 6–7 weeks of age. The

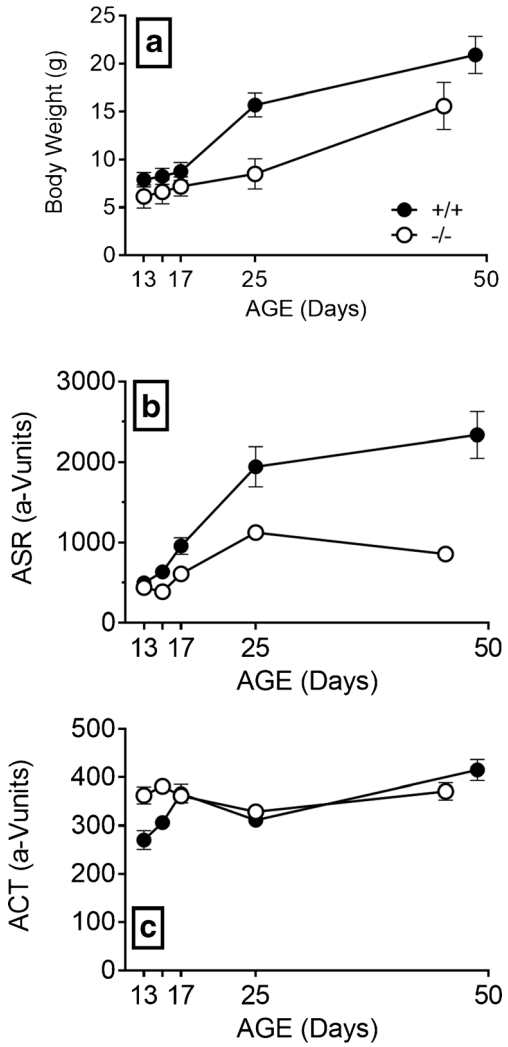

FIG. 4. Experiment 4. **a** The $Hcn1^{+/+}$ mice were always heavier than the $Hcn1^{-/-}$ mice. **b** The $Hcn1^{+/+}$ mice responded more vigorously to the startle stimuli, the difference increasing with age. **c** On P13, the $Hcn1^{-/-}$ mice had more spontaneous activity in the background noise between the test stimuli than the $Hcn1^{+/+}$ mice, with no differences for older mice.

$Hcn1^{+/+}$ mice were always about 30 % heavier than the $Hcn1^{-/-}$ mice, beginning on the first day with a difference of 1.8 (0.38) g, $t(27) = 4.80$, $p < 0.01$, $R^2 = 0.46$, and on the last day a difference of 5.4 (0.81) g, $t(30) = 6.50$, $p < 0.001$, $R^2 = 0.58$. ASR amplitudes were smaller in the $Hcn1^{-/-}$ mice on every day except P13, but this was an artifact of these mice having relatively high levels of spontaneous activity in the time window for the ASR. The ASR of the $Hcn1^{+/+}$ mice was 65 % greater than that of $Hcn1^{-/-}$ mice on P15, Welch's $t(13.53) = 3.41$, $p < 0.01$, $R^2 = 0.46$, and at 6–7 weeks of age, the ASR for the $Hcn1^{+/+}$ mice had increased to almost three times greater than that of the $Hcn1^{-/-}$ mice, Welch's $t(13.41) = 4.99$, $p < 0.001$, $R^2 = 0.65$. It is reasonable to ascribe the less vigorous ASR of the $Hcn1^{-/-}$ mice at least in part to their smaller size, as the correlation between weights and as while ASR amplitudes for the adult mice in each group separately were "near significant" for both $Hcn1^{+/+}$ mice ($r = +0.53$, $p = 0.061$) and $Hcn1^{-/-}$ mice ($r = +0.45$, $p = 0.054$): when these coefficients were combined after transformed to Fishers z, the average correlation was significant, $r = +0.49$, $p < 0.01$, $R^2 = 0.24$.

Figure 5 depicts the increasing levels of PPI across days and across gap durations in the development phase of this experiment. The durations are presented in blocks, the PPI mean for 1 and 2 ms gaps is shown in Fig. 5a; the PPI mean for 3, 4, and 5 ms in Fig. 5b; and PPI mean for 6, 8, 10, and 15 ms in Fig. 5c. Figure 5d depicts the PPI levels for the last pretraining test on P25, in which a constant 10 ms gap was presented at lead times from 10 to 300 ms before the ES. The numbers of mice included in these analyses increased with age and development, older mice being more likely to meet the inclusion criterion. From P13 to P25, the percentages of the included $Hcn1^{+/+}$ mice vs. $Hcn1^{-/-}$ mice were 62 vs. 26, 85 vs. 42, and 100 vs 78 %, and on P25, 100 % in both groups. The numbers of mice for each of the two groups that were included vs. non-included on these days were analyzed by Fisher's exact test; the difference between $Hcn1^{+/+}$ and $Hcn1^{-/-}$ mice was "near significant" for P13 ($p = 0.066$) and significant for P15 ($p = 0.03$). PPI values increased with age and with the duration of the gap (Fig. 5a–c).

The only effect of gene deletion was in the combined performance at the 1–2-ms gap durations and, further, only on P25 (Fig. 5a). The ANOVA had both gene deletion ($Hcn1^{+/+}$ vs. $Hcn1^{-/-}$) and test days (P13, P15, P17, and P25) treated as between-S variables because not all of the mice were tested on every day, while gap duration was the within-S variable. The main effect of gap duration was significant, $F(2/168) = 54.48$, $p = 0.001$, ${}_p\eta^2 = 0.39$, as was the main effect of age, $F(3/84) = 7.34$, $p < 0.001$, ${}_p\eta^2 = 0.21$, as well as the gap duration × age interaction, $F(6/168) = 3.76$, $p = 0.002$, ${}_p\eta^2 = 0.12$. In contrast, the main effect of gene deletion and its interaction with either age or gap duration all provided $F < 1$. The only significant effect of gene deletion appeared in a three-way interaction, with age and the linear trend of gap duration, $F(3/84) = 2.86$, $p = 0.042$, ${}_p\eta^2 = 0.09$.

An overall group threshold was calculated as the smallest duration that significantly inhibited the group mean ASR. On P25, this threshold was 2 ms for the $Hcn1^{+/+}$ group, with a mean PPI of 0.19 (0.05), $p < 0.001$, while for the $Hcn1^{-/-}$ mice the threshold was 3 ms, with a mean PPI level of 0.18 (0.06), $p < 0.02$. Across the series of gap durations, the PPI levels of the two

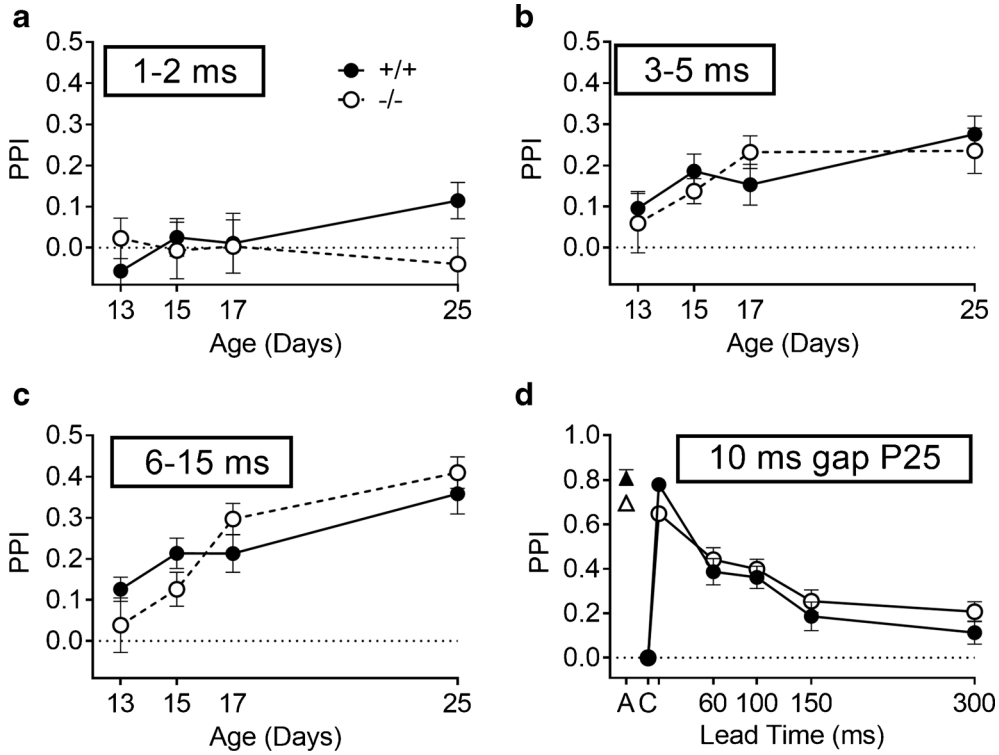

FIG. 5. Experiment 4. Maturation of the inhibitory effects on the ASR (PPI) is shown for increasing gap durations in noise. **a** Combined 1 and 2 ms durations. **b** Combined 3, 4, and 5 ms durations. **c** Combined 6, 8, 10, and 15 ms gap durations. The levels of PPI increased with age and gap duration, but the only significant difference between the $Hcn1^{+/+}$ and $Hcn1^{-/-}$ mice appeared at P25 for the combined durations of 1 and 2 ms. **d** The levels of PPI for the gap pretraining experiment in which the gap was always 10 ms in duration, and the probe startle onset is presented at various interstimulus intervals between 10 and 300 ms. *C* on the abscissa provides the baseline ASR control level, by definition always at "PPI = 0," and *A* is the activity measure in the absence in the eliciting stimulus, which provides the maximum possible level for PPI. The measured PPI for the 10 ms gap that ends with the onset of the ES was close to this maximal potential effect in each group.

groups were significantly different only at 2 ms, with $t(30) = 2.39$, $p = 0.024$, $R^2 = 0.16$. The pretraining data for P25 shown in Fig. 5d describe the recovery from a 10-ms gap after the resumption of the noise background. The offset of noise at the 10-ms interval depressed the ASR to approximate the level of the background activity, revealing a near complete elimination of the ASR by noise offset in both groups, the same effect shown in experiment 3. The subsequent recovery of the ASR was not fully completed by 300 ms, and although there was a trend for a slower recovery in $Hcn1^{-/-}$ mice, there were no significant differences between the groups.

The PPI data for these same mice as adults are shown in Fig. 6. The subjects included 12 $Hcn1^{+/+}$ mice and 19 $Hcn1^{-/-}$ mice, one $Hcn1^{+/+}$ mouse being excluded because of a non-significant ASR on each of the two test days. The group data for the $Hcn1^{+/+}$ mice are similar to those of young adult CBA/CaJ mice (Barsz et al. 2002) and C3HeB/Fej mice (Allen et al. 2008) in showing significant PPI for a 1-ms gap and then an increase to asymptotic levels at 4 to 6 ms. The ANOVA of these data provided a significant main effect for gap duration, $F(8/232) = 36.50$, $p = 0.001$, ${}_p\eta^2 = 0.56$, and a significant interaction of gap duration and gene deletion, $F(8/232) = 6.84$, $p = 0.001$, ${}_p\eta^2 = 0.19$, but the main effect of gene deletion was not significant, $F < 1.0$. The difference between the $Hcn1^{+/+}$ and $Hcn1^{-/-}$ mice was present only for the 1 and 2 ms gaps: for 1 ms, $t(29) = 2.11$, $p = 0.043$, $R^2 = 0.13$; and for 2 ms, $t(29) = 4.28$, $p = 0.001$, $R^2 = 0.39$. The relatively higher asymptotic level of PPI favoring the $Hcn1^{-/-}$ mice at 6 to 15 ms was not significant, $p = 0.14$, $R^2 = 0.07$. The gap threshold was calculated for each mouse as the first gap duration that significantly reduced the ASR below its control level ($\alpha = 0.05$, one tail). For the $Hcn1^{+/+}$ mice, the mean of these individual gap thresholds was 2.17 (0.27) ms, and for the $Hcn1^{-/-}$ mice the threshold was 3.00 (0.17) ms: $t(29) = 2.74$, $p = 0.01$, $R^2 = 0.21$. The ~1 ms difference in gap thresholds between the groups approximates the temporal differences found in experiments 2 and 3, but this is perhaps not surprising, as in vivo electrophysiological experiments report similar gap detection thresholds from the auditory nerve in the chinchilla (Zhang et al. 1990; observed as a cessation of firing within a 2-ms gap) and single cells of the inferior colliculus in the mouse

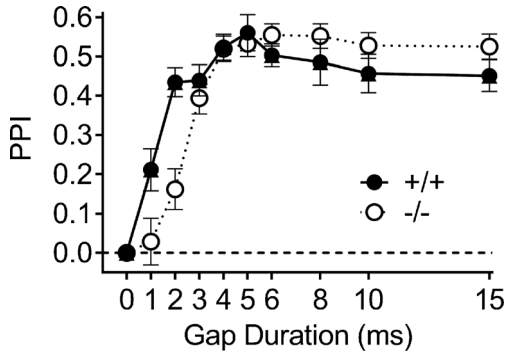

FIG. 6. Experiment 4. The duration of the gap varied between 0 and 15 ms, and the end of the gap was presented at a fixed 60 ms ISI before the startle stimulus. The *Hcn1*$^{+/+}$ mice were more sensitive to brief gaps of 1 and 2 ms, but the groups were not significantly different in their sensitivity to longer gaps.

(Walton et al. 1997, neural firing for Phasic and ON cells at the noise onset at the end of a 2-ms gap).

The more robust ASR amplitude of the *Hcn1*$^{+/+}$ mice was significant from the beginning of the experiment, and while in part, this must reflect the difference in body weight and possibly physical strength, it may also reflect a loss of bilateral summation in the ASR reflex pathways, as shown in the comparable ASR levels in *Kcna1*$^{+/+}$ mice and *Kcna1*$^{-/-}$ mice in monaural listening shown by Karcz et al. (2015). In contrast, the same increasing developmental course of sensitivity to gaps in the *Hcn1*$^{+/+}$ and *Hcn1*$^{-/-}$ mice shown in Fig. 5 is likely to be reflecting the common maturation of synaptic connectivity, receptor sensitivity, and transmitter systems in the auditory brainstem as described, for example, by Sanes and Walsh (1998). The additional benefit of HCN1 ion channels for temporal processing may be evident only after these other mechanisms are in place, seemingly relatively late in the maturation of the auditory system. This last observation appears to be consistent across species, as least for mice and humans, as slow maturation of temporal acuity in young human listeners has been reported by Davis and McCroskey (1980), which follows a near linear improvement of gap detection thresholds with age, beginning with 22 ms for 3-year-olds and ending with 4 ms for 10-year-olds.

Experiment 5

The sound localization experiment might be most difficult for the *Hcn1*$^{-/-}$ mice because the effects of neural asynchrony in monaural pathways would be exacerbated by the demands by spatial acuity for coincident inputs to the bilateral monaural pathways at the binaural nuclei and then their further coincidence with proprioceptive and vestibular inputs for head and body position. Figure 7a shows the disparate PPI performance of the two groups for the 45° separation. For the *Hcn1*$^{+/+}$ mice, there was a more rapid growth of PPI up to a brief plateau at ISI of 30 to 60 ms that was followed by a gradual decline, while PPI for the *Hcn1*$^{-/-}$ mice increased more slowly to a lower asymptotic level that was then maintained to match the PPI level of the *Hcn1*$^{+/+}$ mice at the 300 ms ISI. The ANOVA of the 45° data provided significant main effects for ISI, $F(10/200) = 15.54$, $p < 0.001$, ${}_p\eta^2 = 0.56$, with significant linear and quadratic trends ($p < 0.001$); for gene deletion, $F(1/20) = 13.53$, $p = 0.001$, ${}_p\eta^2 = 0.40$; and a significant interaction between gene deletion and ISI, $F(1/20) = 8.057$, $p = 0.01$, ${}_p\eta^2 = 0.29$. Similar effects (not shown) were obtained at 22.5° and 15° with significant effects for ISI ($p < 0.001$), gene deletion ($p < 0.02$), and their interaction ($p < 0.01$). At 90°, the main effect of ISI was significant, $F(10/200) = 25.44$, $p = 0.001$, ${}_p\eta^2 = 0.56$, but the main effect of gene deletion was not, $F(1/20) = 1.07$, $p = 0.31$, ${}_p\eta^2 = 0.05$. Instead, there was a significant interaction of gene deletion × ISI at 90°, $F(10/200) = 4.52$, $p < 0.001$, ${}_p\eta^2 = 0.18$: contrary to the other conditions, for this 90° stimulus, the *Hcn1*$^{-/-}$ mice had a higher peak PPI. The ANOVA for PPI at the 3.5° angle found no significant effects, with $F < 1$ for both ISI and the ISI × gene deletion interaction, and the main effect of gene deletion was not significant, $F(1/20) = 2.33$, $p = 0.143$.

Figure 7b depicts the group mean performance at the plateau with ISI between 30 and 60 m at each angular separation. The ANOVA of these data provided significant main effects for angular separation, $F(4/80) = 19.14$, $p < 0.001$, ${}_p\eta^2 = 0.49$; for gene deletion, $F = 15.19$, $p = 0.001$, ${}_p\eta^2 = 0.66$; and a significant angular separation x gene deletion interaction, $F(4/80) = 9.44$, $p < 0.001$, ${}_p\eta^2 = 0.32$. The two groups were not different at 3.5° ($p = 0.18$, $R^2 = 0.09$), while PPI for the *Hcn1*$^{+/+}$ mice was significantly higher at 15°, 22.5°, and 45° (all $p < 0.001$ and all $R^2 > 0.45$), and at 90°, the PPI for the *Hcn1*$^{-/-}$ mice was marginally higher than that of the *Hcn1*$^{+/+}$ mice, with Welch's $t(12.4) = 2.04$, $p = 0.06$, $R^2 = 0.25$. The MAA thresholds for each mouse were defined as the smallest angular separation that provided a significant difference ($\alpha < 0.5$, one tail) between the means of the control ASR and the mean ASR at the 30–60 ms plateau; for the *Hcn1*$^{+/+}$ mice, the mean MAA was 29.8° (4.22°), and for the *Hcn1*$^{-/-}$ mice, the mean MAA was 75.17° (6.43°). This difference was significant, $t(20) = 5.64$, $p < 0.001$, $R^2 = 0.61$.

Figure 8 depicts the mean PPI for the two stimulus carriers with 48 and 24 kHz low pass cutoffs in the *Hcn1*$^{+/+}$ and *Hcn1*$^{-/-}$ mice. Both groups detected the 45° change in the position of the stimulus, though the performance of the *Hcn1*$^{+/+}$ mice was better than that

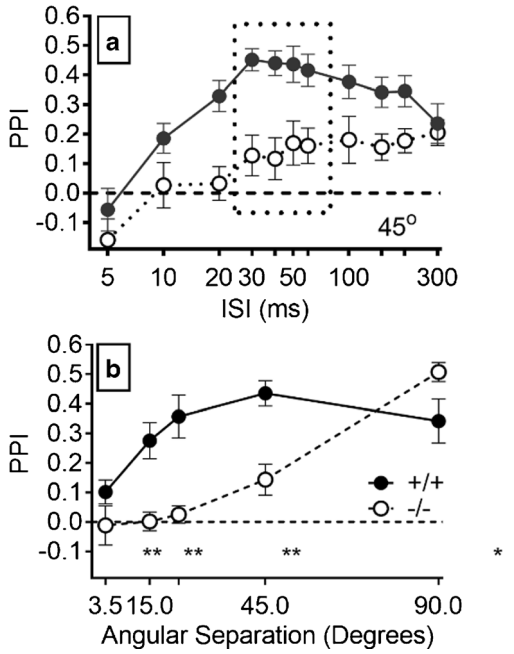

FIG. 7. Experiment 5A. **a** PPI produced by the 45° change in angular separation for the $Hcn1^{+/+}$ and $Hcn1^{-/-}$ mice for different time intervals between the speaker change in location and the startle probe. PPI levels for the $Hcn1^{+/+}$ mice rose rapidly to an asymptotic level at 30–60 ms then gradually declined, while PPI levels for the $Hcn1^{-/-}$ mice more slowly increased to a lower level that then persisted for up to 300 ms. **b** The mean asymptotic levels of PPI marked by the dotted rectangle in **a** for each angular separation from 3.5° up to 90°; a*sterisks* mark the significant differences between the two groups provided by *t* tests: $^{**}p < 0.01$; $^{*}p < 0.05$.

of the $Hcn1^{-/-}$ mice. The ANOVA provided a significant main effect for gene deletion, $F(1/28) = 15.917$, $p < 0.001$, ${}_p\eta^2 = 0.36$; a significant ISI effect, $F(4/112) = 14.59$, $p < 0.001$, ${}_p\eta^2 = 0.39$; and a significant interaction of gene deletion and ISI, $F(4/112) = 3.39$, $p = 0.013$, ${}_p\eta^2 = 0.11$. There was no significant effect of carrier frequency in this overall analysis, and the only *post hoc* comparison that was significant was in the $Hcn1^{+/+}$ mice at ISI of 100 and 200 ms, with greater levels of PPI for the 48 kHz carrier, paired $t(14) = 2.475$, $p = 0.027$, $R^2 = 0.30$. Consistent with the outcome shown in Fig. 7, only 4/15 $Hcn1^{-/-}$ mice had an MAA of at least as low as 45° for each carrier, while 14/15 $Hcn1^{+/+}$ mice had an MAA of at least as low as 45° for the 24 kHz carrier, and 13 mice for the 48 kHz carrier, $p < 0.005$ for each comparison. This outcome indicates that the hearing loss of the $Hcn1^{-/-}$ mice was not the cause of their poor spatial acuity, though the small benefit of the higher "low-frequency cutoff" for the $Hcn1^{+/+}$ mice does agree with previous research in showing that a high frequency carrier does improve spatial acuity (Allen and Ison 2010), at least when the two stimuli cross from one side to the other along the frontal azimuth. The present data provide an interesting contrast to those of Lauer et al. (2011) who found no effect on spatial acuity of either bandwidth or high pass vs. low pass noise when both test locations were presented on the same side of the mouse rather than passing over the frontal midline.

Experiment 6

The rationale for this experiment was to quantify the observed lack of coordination and balance in the $Hcn1^{-/-}$ mice in the home cage, as this would affect sound localization by degrading the sensory information about body/head orientation that is necessary for sound localization in the free field (Kanold and Young 2001; Newlands and Perachio 2003; Shore and Zhou 2006). The $Hcn1^{-/-}$ mice exhibited severe deficits in motor coordination. The median latency (and range) to fall for the $Hcn1^{+/+}$ mice was 19 s (0–30), but for the $Hcn1^{-/-}$ mice, the median was 0 s (0–5): just 2 of the 10 $Hcn1^{+/+}$ mice but 9 of the 13 $Hcn1^{-/-}$ mice fell immediately after they were no longer supported on the elevated rod. The Mann-Whitney median test was significant ($p = 0.001$). These data replicate those of Horwitz et al. (2011) in demonstrating a loss of balance in $Hcn1^{-/-}$ mice that they ascribed to the reduction of I_h in the vestibular hair cells, but may also reflect diminished proprioceptive processing of cues for body and head orientation (Acosta et al. 2012). The changes in performance on both stationary and rotating rotarod tests in HCN1 null mice have been associated with to changes in I_h in vestibular, visual, and possibly proprioceptive function (Horwitz et al. 2011). These authors reported that $Hcn1^{-/-}$ mice learned the task over a series of trials on the stationary rod when tested in an illuminated room and finally matched the performance of the $Hcn1^{+/+}$ mice, but when the light was turned off, they all fell off the rod. HCN1 is expressed in

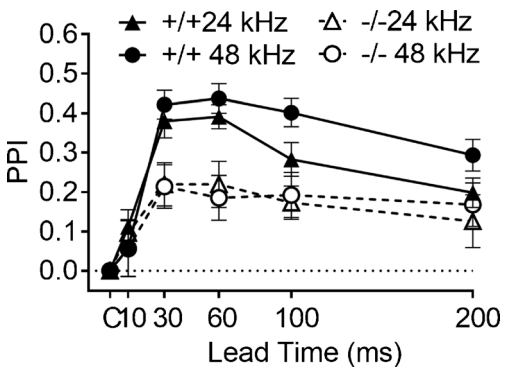

FIG. 8. Experiment 5B. The inhibitory effect of a 45° change in angular separation of 24 or 48 kHz low-pass sounds on the ASR was greater in the $Hcn1^{+/+}$ control mice than those of the $Hcn1^{-/-}$ mice for both stimuli, especially at ISI from 30 to 60 ms.

the superior colliculus and also in the photoreceptors in the retina (Moosmang et al. 1999, 2001). While it seems unlikely that poor bodily orientation would affect measures of monaural temporal acuity, it would more certainly affect sound localization, because vestibular and cutaneous inputs to the auditory nuclei are necessary for discriminating fluctuating binaural disparities in order to disambiguate the external inputs from those resulting from internal head and pinna movements.

SUMMARY AND CONCLUSIONS

In the light of the in vitro observations that showed slowing of brainstem and midbrain auditory neurons when HCN1 is deleted (Cao and Oertel 2011), we expected that deleting this gene in mice could alter both ABR thresholds and waveforms and impair the performance of behaviors governed by fluctuating or transitory acoustic stimuli. Indeed, these mutant mice provide the opportunity to test directly the hypothesis that changing these biophysical properties of neurons would affect hearing in mice.

We have documented eight observations: (1) There were no differences in ABR thresholds of $Hcn1^{+/+}$ and $Hcn1^{-/-}$ mice at the lower spectral frequencies, but thresholds were higher at test frequencies of 32 and 48 kHz in the $Hcn1^{-/-}$ mice (Fig. 1a).This effect may reflect the loss of *Hcn1* channels in the cochlea hair cells. (2) The descending limb of P1 was delayed and P2 was much diminished at 16 kHz, the near "best frequency" for mice, suggesting both a delay and less synchronous firing at the first stage of the brainstem auditory pathways in $Hcn1^{-/-}$ mice (Fig. 1b). (3) Temporal integration of two brief startle-eliciting stimuli was delayed by 1 to 2 ms in the $Hcn1^{-/-}$ mice and reduced in magnitude, consistent with a delay and less synchronous neural firing in the ASR pathways (Fig. 2). (4) The time constants for depression of the ASR by 1 to 10 ms abrupt or gradual noise offsets were about twice as long in the $Hcn1^{-/-}$ mice, and there was a 1-ms delay in the behavioral separation of the abrupt from the ramped offsets. This observation presumably reflects a slower and ragged neural response to acoustic offsets (Fig. 3). (5) Gap detection was measured in juvenile and adult mice by using gaps of different durations to inhibit the ASR. There was no difference between $Hcn1^{-/-}$ and $Hcn1^{+/+}$ mice in their increasing sensitivity to gaps in early development, but at the time of weaning and then as adults, the gap thresholds were lower in the $Hcn1^{+/+}$ mice, at 2.2 ms compared to 3.0 ms in the $Hcn1^{-/-}$ mice (Figs. 5 and 6). The late emergence of the ~1 ms deficit in gap thresholds produced by HCN1 deletion may reflect the relatively slow developmental course of temporal acuity that is seen in both mice and humans. (6) Spatial acuity was very much reduced in mutant mice, with $Hcn1^{-/-}$ mice having a threshold of 75° and the $Hcn1^{+/+}$ mice a threshold of 29° (Fig. 7). This difference was not the result of their poor high frequency hearing because the effect was replicated when both strains were tested with low-pass noise, with either 24 or 48 kHz cutoffs (Fig. 8). (7) A vestibular/proprioceptive processing deficit from HCN1 deletion found in experiment 6 may have compounded the effects on auditory processing in measures of spatial acuity, accounting for the greater effect of HCN1 deletion on spatial localization, compared to monaural temporal acuity. (8) Both body weight and ASR amplitudes were reduced in the $Hcn1^{-/-}$ mice, and significant positive correlations between these two measures indicate that their reduced size and possibly reduced muscular strength contribute to lower ASR levels in $Hcn1^{-/-}$ mice. An additional explanation of the reduced ASR levels in $Hcn1^{-/-}$ mice may reflect the loss of integration in the ipsi- and contralateral startle reflex pathways in the CRN, an effect suggested by Karcz et al. (2015) to explain the higher ASR levels in $Kcna^{+/+}$ mice compared to $Kcna1^{-/-}$ mice, which is found in binaural but not monaural listening conditions. One additional support for the importance of HCN1 for robust sound localization is offered by the auditory effects on their inhabitants of living in a subterranean environment that offers no cues for sound localization. At least one of these mammals, the naked mole-rat, has very poor sensitivity for differences in spatial position (Heffner and Heffner 1993); this coupled with a lack of HCN1 in the binaural brainstem (Gessele et al. 2016).

Relevant caveats for our understanding of these observations have been mentioned above, including the possibility that various types of compensation might mask the full contribution of HCN1 deletion to auditory processing or that the deleterious effects of HCN1 deletion on other sensory or motor systems may have an additional impact on behavior and thus exaggerate its effects on auditory processing. For the first caveat, there are likely compensatory changes in other members of the HCN family as well as changes in other neural mechanisms following HCN1 deletion, but they must not be completely effective because the observations of changes in evoked potentials and in behavior are at least at the qualitative level consistent with the data of in vitro experiments. For the second caveat, the effects of HCN1 deletion on sound localization are certainly not entirely due to diminished auditory processing, because spatial acuity depends also on proprioceptive, vestibular, and cutaneous pathways that also express HCN1. An additional technical issue is raised by the effect of HCN1 deletion on the vigor of the ASR because this partially motor deficit could possibly compromise PPI as a measure of sensory processing. But in defense of this behavioral/psychophysical procedure, Fechter and Young (1983) observed stable PPI measures of sensitivity

to auditory stimuli before and then after exposure to triethyltin, which is a neuromuscular toxicant that reduced the control level of the ASR in rats by 80 %.

In conclusion, we found that the behaviors that depend on the presence of HCN1 include balance and motor coordination; the vigorous startle responses that require spatial integration of the simultaneous inputs to both ears and temporal integration for near-simultaneous paired stimuli; the several forms of gap detection that require precisely timed responses to both onsets and offsets of acoustic stimuli; and especially for sound localization, temporal precision across auditory, vestibular, and cutaneous pathways so that neural activity in these pathways arrive in unison at their rostral targets.

ACKNOWLEDGEMENTS

This research was supported by grants from the National Institutes of Health, DC00176, and the Schmitt Foundation for Integrative Brain Research.

COMPLIANCE WITH ETHICAL STANDARDS

All procedures were approved by the University of Rochester Committee on Animal Resources in accord with Public Health Service regulations and the Federal Animal Welfare Act.

REFERENCES

Acosta C, McMullan S, Djouhri L, Gao L, Watkins R, Berry C, Dempsey K, Lawson SN (2012) HCN1 and HCN2 in rat DRG neurons: levels in nociceptors and non-nociceptors, NT3-dependence and influence of CFA-induced skin inflammation on HCN2 and NT3 expression. PLoS ONE [Electronic Resource] 7(12):e50442 e5044

Allen PD, Ison JR (2010) Sensitivity of the mouse to changes in azimuthal sound location: effects of angular separation, spectral composition, and sound level on prepulse inhibition of the acoustic startle reflex. Beh Neurosci 124:265–277

Allen PD, Ison JR (2012) Kcna1 gene deletion lowers the behavioral sensitivity of mice to small changes in sound location and increases asynchronous brainstem auditory evoked potentials, but does not affect hearing thresholds. J Neurosci 32:2538–2543

Allen PD, Schmuck N, Ison JR, Walton JP (2008) Kv1.1 channel subunits are not necessary for high temporal acuity in behavioral and electrophysiological gap detection. Hear Res 246:52–58

Bakondi G, Por A, Kovacs I, Szucs G, Rusznak Z (2009) Hyperpolarization-activated, cyclic nucleotide-gated, cation non-selective channel subunit expression pattern of guinea-pig spiral ganglion cells. Neurosci 158:1469–1477

Bal R, Oertel D (2000) Hyperpolarization-activated, mixed-cation current (Ih) in octopus cells of the mammalian cochlear nucleus. J Neurophysiol 84:806–817

Bal R, Oertel D (2001) Potassium currents in octopus cells of the mammalian cochlear nuclei. J Neurophysiol 86:2299–2311

Banks MI, Pearce RA, Smith PH (1993) Hyperpolarization-activated cation current (Ih) in neurons of the medial nucleus of the trapezoid body: voltage-clamp analysis and enhancement by norepinephrine and cAMP suggest a modulatory mechanism in the auditory brain stem. J Neurophysiol 70:1420–1432

Barsz K, Ison JR, Snell KB, Walton JP (2002) Behavioral and neural measures of auditory temporal acuity in aging humans and mice. Neurobiol Aging 23:565–578

Buchtel HA, Stewart JD (1989) Auditory agnosia: apperceptive or associative disorder? Brain Lang 37:12–25

Cao XJ, Oertel D (2011) The magnitudes of hyperpolarization-activated and low-voltage-activated potassium currents co-vary in neurons of the ventral cochlear nucleus. J Neurophysiol 106:630–640

Chen C (1997) Hyperpolarization-activated current (Ih) in primary auditory neurons. Hear Res 110:179–190

Chen X, Shu S, Schwartz LC, Sun C, Kapur J, Bayliss DA (2010) Homeostatic regulation of synaptic excitability: tonic GABA(A) receptor currents replace I(h) in cortical pyramidal neurons of HCN1 knock-out mice. J Neurosci 30:2611–2622

Crawley JN, Belknap JK, Collins A, Crabbe JC, Frankel W, Henderson N, Hitzemann RJ, Maxson SC, Miner LL, Silva AJ, Wehner JM, Wynshaw-Boris A, Paylor R (1997) Behavioral phenotypes of inbred mouse strains: implications and recommendations for molecular studies. Psychopharmacol 132:107–124

Davis SM, McCroskey RL (1980) Auditory fusion in children. Child Dev 51:75–80

Dean KF, Sheets LP, Crofton KM, Reiter LW (1990) The effect of age and experience on inhibition of the acoustic startle response by gaps in background noise. Psychobiol 18:89–95

Dodson PD, Barker MC, Forsythe ID (2002) Two heteromeric Kv1 potassium channels differentially regulate action potential firing. J Neurosci 22:6953–6961

Exner S (1875) Experimentelle untersuchung der einfachsten psychischen processe. Pflugers Arciv 11:403–432 (described in W. James, p613-614, Principles of psychology, Vol 1, 1890)

Fechter LD, Young JS (1983) Discrimination of auditory from nonauditory toxicity by reflex modulation audiometry: effects of triethyltin. Tox Appl Pharmacol 70:216–227

Felix RA, Fridberger A, Leijon S, Berrebi AS, Magnusson AK (2011) Sound rhythms are encoded by postinhibitory rebound spiking in the superior paraolivary nucleus. J Neurosci 31(35):12566–12578

Felix RA II, Magnusson AK, Berrebi AS (2014) The superior paraolivary nucleus shapes temporal response properties of neurons in the inferior colliculus. Brain Struct Funct. doi:10.1007/s00429-014-0815-8

Fettiplace R, Kim KX (2014) The physiology of mechanoelectrical transduction channels in hearing. Physiol Rev 94:951–986

Gessele N, Garcia-Pino E, Omerbašić D, Park TJ, Koch U (2016) Structural changes and lack of HCN1 channels in the binaural auditory brainstem of the naked mole-rat (*Heterocephalus glaber*). PLoS One 11(1):e0146428. doi:10.1371/journalpone0146428

Golding NL, Oertel D (2012) Synaptic integration in dendrites: exceptional need for speed. J Physiol 590:5563–5569

Gomez-Nieto R, Horta-Junior JA, Castellano O, Millian-Morell L, Rubio ME, Lopez DE (2014) Origin and function of short-latency inputs to the neural substrates underlying the acoustic startle reflex. Front Neurosci 8:216

Heffner RS, Heffner HE (1993) Degenerate hearing and sound localization in naked mole rats (*Heterocephalus glaber*), with an overview of central auditory structures. J Comp Neurol 331:418–433

Henry KR (1979) Auditory brainstem volume-conducted responses: origins in the laboratory mouse. J Am Aud Soc 4:173–178

Horwitz GC, Risner-Janiczek JR, Jones SM, Holt JR (2011) HCN channels expressed in the inner ear are necessary for normal balance function. J Neurosci 31:16814–16825

Ison JR, Allen PD (2012) Deficits in responding to brief noise offsets in Kcna1$^{-/-}$ mice reveal a contribution of this gene to precise

temporal processing seen previously only for stimulus onsets. JARO 13:351–358

James W (1890) Principles of psychology, Vol 1. Henry Holt and Company, New York

Kanold PO, Young ED (2001) Proprioceptive information from the pinna provides somatosensory input to cat dorsal cochlear nucleus. J Neurosci 21:7848–7858

Karcz A, Allen PD, Walton J, Ison JR, Kopp-Scheinpflug C (2015) Auditory deficits of Kcna1 deletion are similar to those of a monaural hearing loss. Hear Res 321:45–51

Khurana S, Remme MWH, Rinzel J, Golding NL (2011) Dynamic interaction of Ih and IK-LVA during trains of synaptic potentials in principal neurons of the medial superior olive. J Neurosci 31(24):8936–8947

Khurana S, Liu Z, Lewis AS, Rosa K, Chetkovich D, Golding NL (2012) An essential role for modulation of hyperpolarization-activated current in the development of binaural temporal precision. J Neurosci 32:2814–2823

Kim YH, Holt JR (2013) Functional contributions of HCN channels in the primary auditory neurons of the mouse inner ear. J Gen Physiol 142:207–223

Koch U, Braun M, Kapfer C, Grothe B (2004) Distribution of HCN1 and HCN2 in rat auditory brainstem nuclei. Eur J Neurosci 20:79–91

Kopp-Scheinpflug C, Tozer AJ, Robinson SW, Tempel BL, Hennig MH, Forsythe ID (2011) The sound of silence: ionic mechanisms encoding sound termination. Neuron 71:911–925

Lauer AM, Slee SJ, May BF (2011) Acoustic basis of directional acuity in laboratory mice. JARO 12:633–645

Manis PB, Marx SO (1991) Outward currents in isolated ventral cochlear nucleus neurons. J Neurosci 11:2865–2880

Marsh R, Hoffman HS, Stitt CL (1973) Temporal integration in the acoustic startle reflex of the rat. J Comp Physiol Psychol 82:507–511

Melcher JR, Kiang NY (1996) Generators of the brainstem auditory evoked potential in cat. III: identified cell populations. Hear Res 93:52–71

Michalewski HJ, Starr A, Nguyen TT, Kong YY, Zeng FG (2005) Auditory temporal processes in normal-hearing individuals and in patients with auditory neuropathy. Clin Neurophysiol 116:669–680

Mills AW (1958) On the minimum audible angle. J Acoust Soc Am 30:237–246

Mo ZL, Davis RL (1997) Heterogeneous voltage dependence of inward rectifier currents in spiral ganglion neurons. J Neurophysiol 78:3019–3027

Moosmang S, Biel M, Hofmann F, Ludwig A (1999) Differential distribution of four hyperpolarization-activated cation channels in mouse brain. Biol Chem 380:975–980

Moosmang S, Stieber J, Zong X, Biel M, Hofmann F, Ludwig A (2001) Cellular expression and functional characterization of four hyperpolarization-activated pacemaker channels in cardiac and neuronal tissues. Eur J Biochem 286:1646–1652

Newlands SD, Perachio AA (2003) Central projections of the vestibular nerve: a review and single fiber study in the Mongolian gerbil. Brain Res Bull 60:475–495

Oertel D, Shatadal S, Cao XJ (2008) In the ventral cochlear nucleus Kv1.1 and subunits of HCN1 are colocalized at surfaces of neurons that have low-voltage-activated and hyperpolarization-activated conductances. Neurosci 154:77–86

Ramakrishnan NA, Drescher MJ, Khan KM, Hatfield JS, Drescher DG (2012) HCN1 and HCN2 proteins are expressed in cochlear hair cells: HCN1 can form a ternary complex with protocadherin 15 CD3 and F-actin-binding filamin A or can interact with HCN2. J Biol Chem 287:37628–37646

Sanes DH, Walsh EJ (1998) The development of central auditory processing. In: Rubel EW, Popper AN, Fay RR (eds) Development of the auditory system. Springer, NY, pp. 271–314

Shore SE, Zhou J (2006) Somatosensory influence on the cochlear nucleus and beyond. Hear Res:216–217 90-99

Snell KB, Mapes FM, Hickman ED, Frisina DR (2002) Word recognition in competing babble and the effects of age, temporal processing, and absolute sensitivity. J Acoust Soc Am 112:720–727

Starr A, Zaaroor M (1990) Eighth nerve contributions to cat auditory brainstem responses (ABR). Hear Res 48:151–169

Wahl-Schott C, Biel M (2009) HCN channels: structure, cellular regulation and physiological function. Cell Mol Life Sci 66:470–494

Walton JP, Frisina RD, Ison JR, O'Neill WE (1997) Neural correlates of behavioral gap detection in the inferior colliculus of the young CBA mouse. J Comp Physiol A 181:161–176

Wang Y, Manis BP (2008) Short-term synaptic depression and recovery at the mature mammalian endbulb of Held synapse in mice. J Neurophysiol 100:1255–1264

Yang H, Xu-Friedman MA (2009) Impact of synaptic depression on spike timing at the endbulb of Held. J Neurophysiol 102:1699–1710

Yi E, Roux I, Glowatzki E (2010) Dendritic HCN channels shape excitatory postsynaptic potentials at the inner hair cell afferent synapse in the mammalian cochlea. J Neurophysiol 103:2532–2543

Yoshida N, Hequembourg SJ, Atencio CA, Rosowski JJ, Liberman MC (2000) Acoustic injury in mice: 129/SvEv is exceptionally resistant to noise-induced hearing loss. Hear Res 141:97–106

Zeng FG, Kong YY, Michalewski MJ, Starr A (2005) Perceptual consequences of disrupted auditory nerve activity. J Neurophysiol 93:3050–3063

Zhang W, Salvi RJ, Saunders SS (1990) Neural correlates of gap detection in auditory nerve fibers of the chinchilla. Hear Res 46:181–200